Bioactive Materials 30 (2023) 85–97

Contents lists available at ScienceDirect

Bioactive Materials

journal homepage: www.keaipublishing.com/en/journals/bioactive-materials

Bionic peptide scaffold in situ polarization and recruitment of M2 macrophages to promote peripheral nerve regeneration

Pengxiang Yang [a,b], Yong Peng [a], Xiu Dai [a], Jing Jie [c,**], Deling Kong [d], Xiaosong Gu [a,***], Yumin Yang [a,*]

[a] Key Laboratory of Neuroregeneration of Jiangsu Province and Ministry of Education, Co-Innovation Center of Neuroregeneration, NMPA Key Laboratory for Research and Evaluation of Tissue Engineering Technology Products, Nantong University, 226001, Nantong, PR China
[b] Institute of Cancer Prevention and Treatment, Heilongjiang Academy of Medical Science, Harbin Medical University, 150081, Harbin, PR China
[c] Department of Clinical Laboratory, The Second Affiliated Hospital of Nantong University, 226001, Nantong, PR China
[d] State Key Laboratory of Medicinal Chemical Biology, College of Life Sciences, Nankai University, Tianjin, 300071, PR China

ARTICLE INFO

Keywords:
Bionic peptide scaffolds
Peripheral nerve regeneration
Macrophages
Conditional media
Immune microenvironment

ABSTRACT

Tissue regeneration requires exogenous and endogenous signals, and there is increasing evidence that the exogenous microenvironment may play an even more dominant role in the complex process of coordinated multiple cells. The short-distance peripheral nerve showed a spontaneous regenerative phenomenon, which was initiated by the guiding role of macrophages. However, it cannot sufficiently restore long-distance nerve injury by itself. Based on this principle, we firstly constructed a proinflammatory model to prove that abnormal M2 expression reduce the guidance and repair effect of long-distance nerves. Furthermore, a bionic peptide hydrogel scaffold based on self-assembly was developed to envelop M2-derived regenerative cytokines and extracellular vesicles (EVs). The cytokines and EVs were quantified to mimic the guidance and regenerative microenvironment in a direct and mild manner. The bionic scaffold promoted M2 transformation in situ and led to proliferation and migration of Schwann cells, neuron growth and motor function recovery. Meanwhile, the peptide scaffold combined with CX3CL1 recruited more blood-derived M2 macrophages to promote long-distance nerve reconstruction. Overall, we systematically confirmed the important role of M2 in regulating and restoring the injury peripheral nerve. This bionic peptide hydrogel scaffold mimicked and remodeled the local environment for M2 transformation and recruitment, favoring long-distance peripheral nerve regeneration. It can help to explicate regulative effect of M2 may be a cause not just a consequence in nerve repair and tissue integration, which facilitating the development of pro-regenerative biomaterials.

1. Introduction

Tissue regeneration requires exogenous and endogenous signals from multiple cell types, with temporal coordination and dynamic reprogramming changes [1]. Most tissues of the human body lack spontaneous regeneration after injury; in some cases, this is largely explained by endogenous signals, such as insufficient sources of stem cells [2,3]. However, more evidence has revealed that the exogenous microenvironment may play an even more dominant role in the complex process of coordinated regeneration of multiple cells [4,5]. The peripheral nervous system is one of the most important regenerative tissues and research model of the human body due to its regenerative phenomenon [6].

Complete peripheral nerve transection commonly occurs in medical and traffic accidents. The injured nerve fibers lead to the loss of motor activity and sensation in the respective part of the body [7]. The current clinical treatment for short or critical distances is surgical suturing of the ends of stumps, and regeneration relies on the replacement of injured structural cells. In this process, the two stumps are rejoined by change and reconstruction of the microenvironment into the gap and are composed of a mixture of inflammatory cells and matrix [8].

Peer review under responsibility of KeAi Communications Co., Ltd.
* Corresponding author.
** Corresponding author.
*** Corresponding author.
E-mail addresses: jiejing1103@126.com (J. Jie), nervegu@ntu.edu.cn (X. Gu), yangym@ntu.edu.cn (Y. Yang).

https://doi.org/10.1016/j.bioactmat.2023.07.003
Received 4 May 2023; Received in revised form 19 June 2023; Accepted 4 July 2023

Macrophages are considered to be the most important immune effector cells because they show plasticity that allows them to react to tissue-specific signals while retaining the ability to execute core functions as tissue phagocytes [9,10].

After peripheral nerve injury, the stumps retract generating a gap of several millimeters. The injured myelin and distal axons rapidly degenerate due to detachment from the neuron bodies and activate the process of Wallerian degeneration [11]. Macrophages are the main effector cells responsible for the removal of damaged cell debris, and they show the classically activated phenotype and strong phagocytosis accompanied by the secretion of proinflammatory cytokines known as M1 macrophages at this stage. Currently, it is generally agreed that the M1-induced inflammatory reaction forms a hostile regenerative microenvironment [12].

Following the removal of debris, inflammation gradually subsides, and a regenerative microenvironment is slowly formed through the cooperation of multiple cells [13]. Macrophages selectively respond to local hypoxia within the gap named the regenerative bridge region, and secreted growth factors triggers polarized vascularization [8]. The newly formed blood vessels play a guiding role in Schwann cell reconnection to the distal ends of stumps, and axons of the regenerative nerve are subsequently formed [14]. At this stage, macrophages change their phenotype by sensing changes in the microenvironment, and the number of alternatively activated M2 macrophages increases. They produce a variety of pro-healing cytokines, further strengthening the regenerative environment and promoting structural cell growth [15–17]. M1-inflammation and M2-regeneration are interdependent and overlapping phases. Overall, macrophages are the initiator of endogenous signals of nerve regeneration, even if the time and rate of transformation from M1 to M2 phenotype in injured peripheral nerve regeneration are still unknown.

For long-distance or severe nerve injury, spontaneous nerve regeneration cannot be guided by endogenous signals, and a graft is necessary to bridge the gap between the proximal and distal nerve ends. Autologous nerve grafts are still the standard of bionics research and have the best clinical curative effect; however, they are limited to donor sources and mismatched with the defect sites [18,19]. Alternatively, nerve guidance conduits are trying to reach the “gold standard” with features such as appropriate biocompatibility, degradation rate and adequate mechanical properties [13,20]. The current conduit mainly serves a guiding role, but regenerative nerves do not show sufficient vitality. The microenvironment is an essential element during the whole regeneration process [21]. Macrophages participate in all injured nerve regeneration processes, and they play a regulatory role [9,22]. The precise regulation of macrophage transformation and recruitment events by engineering technology may result in better effects on long-distance peripheral nerve injury.

Here, we constructed a proinflammatory model (*Model 1*) to verify the guidance and repair role of M2 macrophages in long-distance peripheral nerve injury. A bionic peptide hydrogel scaffold based on self-assembly was developed to promote M2 programming transformation in situ (*Model 2*). M2-derived conditioned medium comprised of regenerative cytokines and extracellular vesicles (EVs) was made, and the EVs were quantified and enveloped in hydrogel scaffolds to contribute to the constructive microenvironment, leading to the proliferation and migration of Schwann cells, neuron growth, and recovery of muscle motor function. Furthermore, the bionic peptide hydrogel scaffold was combined with chemokines to recruit blood-derived macrophages to promote functional nerve recovery (*Model 3*). We systematically confirmed the important role of M2 in long-distance peripheral nerve injury and good regenerative effect of bionic peptide hydrogel scaffold remodeling of the local environment for M2 transformation and recruitment in a direct and mild manner.

2. Materials and methods

2.1. Animals

SD adult rats (190 g–210 g) and suckling rats (1d) were received from Nantong University. All experimental and animal handling procedures were performed according to the US National Institute of Health (NIH) guide for the care and use of laboratory animals published by the US national academy of sciences, and approved by the administration committee of experimental animals of Jiangsu Province.

2.2. Schwann cells culture

The sciatic nerve of suckling rats were cut into pieces and ground, hydrolyzed by 1% collagenase for 30 min, and then hydrolyzed in 0.25% trypsin (Roche, IN, USA) at 37 °C for 5–8 min. Digestion was terminated with high glucose DMEM containing 10% fetal bovine serum, followed by centrifugation at 1200 r/min for 5 min. Cells were cultured in DMEM containing 10% fetal bovine serum. After 16 h, the medium was added 10 mM cytosine arabinoside. Cells were incubated at 37 °C for 24 h to inhibit the proliferation of fibroblasts. Medium was changed to high glucose medium supplemented with 10% fetal bovine serum, 2 mM forskolin and 2 ng/ml heregulin (Sigma, MO, USA) to stimulate Schwann cell proliferation. The cell density occupied about 90% of the bottom area of the culture dish, and peeled with 0.25% trypsin. Schwann and Anti-thy 1.1 antibody (1:1000) were incubated at 4 °C for 2 h, and reacted with complement (Jackson, PA, USA) at 37 °C for 30 min to clear fibroblasts.

2.3. M2 macrophages culture

The macrophages were received from SD rat ascitic fluid. After cervical dislocation, adult rats were immersed in 75% alcohol for sterilize and then pre-prepared PBS was injected into the abdominal cavity. The abdomen was massaged gently for 3–5 min. Remove the abdominal fluid and centrifuge at 1000 r/min for 10 min. Cells were cultured in a medium containing 10% fetal bovine serum and 10 ng/ml IL-4 to polarize into M2 macrophages. The supernatant was collected known as M2-conditioned medium for subsequent experiments, and store at −80 °C.

2.4. Cell viability assay

The cells were plated in 24-well and cultured at 37 °C for 24 h. Then the supernatant was removed and cleaned with PBS for 3 times. Each well was added with 0.3 μL Calcein AM and PI, incubated at 37 °C for 30 min away from light. The living cells (Green) and dead cells (Red) were observed by fluorescence microscopy.

2.5. Cell proliferation experiment

RSC96 were cultured in 24-well plates with a density of 30%, and the cells were divided into four groups. There are media, M2-conditioned medium, scaffold and bionic scaffold group. The dilute Edu solution (1:1000) was mixed with cells and cultured at 37 °C for 4 h. The cells was fixed in 4% polyformaldehyde at 25 °C for 30 min and permeated with PBS solution which containing 0.3% TritonX-100 for 15 min. Then cells were observed under confocal microscope (Leica TCS SP5).

2.6. Cell migration experiment

The isolation chambers were attached the bottom of the 12-well plate, and the cells were added. Take pictures with transmitted light at 2, 4, 8, 12 and 24 h respectively, and record the migration distance of cells. The migration distance is the absolute value of the gap between two cells minus the gap at the beginning of migration.

2.7. Luminex multiplex array

The cell supernatant was collected and removed particulates by centrifugation. Array buffer was added into 4-well multi-dish serving as a block buffer. Place membrane into 4-well multi-dish with the number facing upward. Incubate for 1 h on a rocking platform shaker. Add 15 μL detection antibody cocktail to the sample and incubate at room temperature for 1 h. Then aspirate array buffer and add prepared sample. Incubate overnight at 4 °C on a rocking platform shaker. Wash the membrane with wash buffer for 10 min on a rocking platform shaker for three times. Add the membrane into 2 mL of diluted streptavidin-HRP of the 4-well multi-dish. Incubate for 30 min at room temperature on a rocking platform shaker. Lay chemi-reagent mix on the membrane and expose to X-ray film for 1–10 min.

2.8. Real-time quantitative PCR analysis

Total RNA was collected and the ratio of A260:A280 was used to indicate the purity. Complementary DNA (cDNA) was generated using the First Strand cDNA Synthesis kit, according to the manufacturer's instructions. qRT-PCR was performed with SYBR-Green PCR Master Mix (Roche, Basel, Switzerland) and Applied Biosystems 7500 Fast System (ABI, CA, USA). Relative levels of gene expression were determined with GAPDH as the control.

2.9. ELISA

Cytokines and chemokines were assayed by ELISA, 100 μL of standard sample or experimental sample were added into each well and incubated at 37 °C for 90 min. After the liquid was removed, detected antibody was added into each well and incubated 60 min. After the solution was removed, 100 μL enzyme-bound substrate was added and incubated at 37 °C for 30 min. The substrate solution was incubated for 15 min, then the termination solution was added. OD value was measured at 450 nm by spectrophotometer.

2.10. Immunofluorescence staining analysis

The sciatic nerve on the surgical side was taken out and the part of regenerated nerve in the silicone tube was preserved. The tissue was cut transversely or longitudinally into pieces in frozen microtome and then dried. S100 (Abcam, ab52642), Tuj-1 (Abcam, ab25770) or CD206 rabbit (Proteintech, 18704-1-AP) were selected as the first antibody and incubated at 4 °C for 12 h. CY-3 anti-rabbit (Abcam, ab6939) was the second antibody, and were observed under a confocal microscope.

2.11. Flow cytometry

Cells were digested with 0.25% trypsin and fixed with 4% paraformaldehyde for 30 min. After the cells were washed with PBS for three times, they were incubated with the fluorescently-labeled antibody for 1 h at room temperature, and then the positive cells were detected. *In vivo* study, the silicone tube on the surgical side was taken out and the liquid in the tube was collected in 1 ml of PBS. The total number of positive cells were detected by flow cytometry.

2.12. Animal models

Proinflammatory model: adult rats were randomly divided into natural group (PBS) and inflammatory group (Mix agonist, 1 μg/μL CpG ODNs + 1 μg/μL LPS) was injected into a silicone tube. The sciatic nerve tissue preparation animals were anesthetized by intraperitoneal injection of a combined anesthetic solution of sodium pentobarbital and chloral hydrate (0.3 mL/100 g). The left sciatic nerve was exposed by incising the skin and splitting the muscle. A segment of the sciatic nerve was cut and excised, and the defect was 7-mm. Then, the proximal and distal ends of the sciatic nerve were connected with a silicone tube and sutured with 7-0 surgical suture, and the muscle tissue and skin wound were closed with 4-0 surgical suture.

Bionic scaffold model: adult rats were randomly divided into autograft group, media group, M2-conditioned medium group (M2-C), scaffold group (Scaffold) and bionic scaffold group (Bio-scaffold). The nerve stumps were transected to create 10-mm nerve defects and each group was injected with 30 μL of media or hydrogel. The surgical procedure and experimental methods were the same as above.

Recruitment experiment model: adult rats were randomly divided into autograft group, MCP-1 or CX3CL1 was enveloped in bionic scaffold group, and macrophages were depleted using clodronate liposomes (Inhibitor). Media and bionic peptide scaffold served as control group. The nerve stumps were transected to create 12-mm nerve defects and each group was injected with 30 μL of media or hydrogel. The surgical procedure and experimental methods were the same as above.

2.13. Motor functional analysis and electrophysiological examination

At 8 week after the nerve defect, the footprints were measured by the catwalk system and the sciatic functional index (SFI) was calculated and scored according to the BMS standard. Rats were anesthetized and sciatic nerves on the operative and non-operative sides were re-exposed. Electrical stimulation (10 mV) was sequentially applied to the proximal and distal nerve stumps, and compound muscle action potentials (CMAP) of gastrocnemius were recorded. The CMAP of non-surgical side was known as the normal group and the negative wave amplitudes in the electrophysiological evaluation results of each group were compared. Rats were perfused and the gastrocnemius muscle on the operated side and the non-operated side were taken out. The wet weight ratio in each group was calculate.

2.14. Transmission electron microscopy and HE staining

The regenerated nerve in the nerve conduit was dissociated and detected. The samples were used to measure and count the thickness and the density of regenerated nerve in each experimental group by Image J. The gastrocnemius muscle was fixed in 4% paraformaldehyde and tissue was dissociated from the muscle. The tissues were coated with paraffin, dehydrated with ethanol, and then sliced. The sample slides were stained with hematoxylin solution, eosin solution and then sealed with A-resin.

2.15. Statistical analysis

Standard statistical tests including an unpaired two-tailed student's t-test and one-way ANOVA were used to evaluate the significance. $P < 0.05$ was considered to indicate a statistically significant difference.

3. Results

3.1. Disturbance of the local microenvironment reduced M2 macrophages within the bridge after long-distance peripheral nerve injury

The sciatic nerve was transected and bridged with a tube filled with mixed agonist. Local injured nerves were immersed in an inflammatory state compared with the natural repair group due to high concentrations of agonist, which disturbed programmed regeneration. After injury, macrophages were found to be the most important immune cells in the bridge, and it is well accepted that M2-like macrophages play an important role in tissue regeneration. Flow cytometry analysis showed that the percentages of M2 macrophages (Iba-1^{+}CD206^{+}) were 2.38% and 29.4% at day 3 and 7 after nerve injury in the natural repair group, respectively. It also increased in the inflammation group; however, the percentages were 0% and 5.79% at day 3 and 7. M2 expression was delayed and significantly lower in the early stage of injury, which is

considered the optimal time for damaged tissue repair (Fig. 1A and B). Localization of M2 macrophages via immunofluorescence staining for CD206 was performed. At day 3, more M2 macrophages appeared in the proximal and distal ends of the injured nervous tissue and there were no significant differences in the middle of the bridge (Fig. 1C). At day 7, they were distributed in the whole bridge. The percentage of M2 macrophages was lower and the pro-inflammatory TNF-α was higher in the regenerative process of inflammation group (Fig. 1D and E, Fig. S1). These results indicated that high concentrations of agonist reduced M2 macrophages within the bridge after long-distance peripheral nerve injury. The percentage of M2 macrophages was lower in the middle compared with the two ends of the stumps at the early stage of injury, which indicated a guiding effect on nerve regeneration.

Two weeks after the conduit implantation into the rat sciatic nerve, the length and fluorescence intensity of Schwann cells also significantly decreased in the mixed agonist group (Fig. 2A–C). At the same time, the number of regenerative nerve cells in the mixed agonist group was dramatically reduced by approximately 48% compared to that in the natural control group, confirming that the decreased percentage of M2 macrophages delayed injury sciatic nerve regeneration (Fig. 2D). The middle of the regenerative bridge shows a lower intensity of newly formed tissue, which is consistent with the localization of M2 macrophages. We further evaluated functional recovery after peripheral nerve injury in local excessive inflammation, and the compound muscle action potential (CMAP) of the gastrocnemius muscle was recorded using electromyography 8 weeks after surgery and representative electrophysiological images of the two groups are shown in Fig. 2E. The CMAP amplitude in the mixed agonist group at both the proximal and distal ends of the injured nervous was significantly lower than that in the natural group (Fig. 2F). Gradual achievement of normal gait is also a sign of functional recovery. The sciatic functional index (SFI) was used to analyze rat gait and assess nerve regeneration. Representative footprints from each group are shown in Fig. 2G. The SFI in the natural recovery groups was significantly higher than that in the inflammatory group at 8 weeks (Fig. 2H, Fig. S2). These results indicated that excessive inflammation decreased the expression and guidance of M2 macrophages, leading to worse motor neurologic functional recovery.

3.2. Construction and characterization of bionic peptide hydrogel scaffold

Biomimetic scaffolds are increasingly used to support or reprogram the complex regenerative microenvironment by providing structural stability and mechanical restoration. In our research, the self-assembling peptide FEFEFKFK (FEFK), which is composed of a core of alternating hydrophilic and hydrophobic residues that drive assembly to form hydrogel, was applied as a functional scaffold material. The flanking domains were designed by incorporating the short BDNF mimic peptide IKRG to form a nanoartificial neurotrophic factor, which promoted the rapid regeneration of injured nerves (Fig. 3A, Figs. S3–4). To better form the hydrogel assembly, an equal proportion of FEFK was mixed with nanoartificial factor to form scaffold. Fig. 3B indicates that the scaffold shows a typical β-sheet conformation with minimum and maximum molar ellipticity at 202 nm and 198 nm, respectively. It has been confirmed that such a β-sheet structure is stable over a wide range of temperatures and pH values. The scaffold spontaneously assembled into nanofibers when it was exposed to cell culture media or buffer solution, as shown in the TEM image (Fig. 3C). It developed into long fibers after 12 h, and formation of fiber aggregation or bundles occurred after 72 h. The length of such nanofibers increased with assembly time, and more nanofibrous networks formed via an end-to-end fiber-fiber aggregation mechanism. Nanofibers were singly distributed, and long nanofibers were either singly distributed or aggregated via entanglements.

To further mimicked the complex immune microenvironment, M2-derived conditional medium (M2-C) was enveloped forming bionic peptide scaffold. Fig. 3D shows that M2-C had a large content of regenerative cytokines, including IL-10, IL-1ra, and IL-1β, and chemokines, such as CCL5 and CCL20, which were detected using Luminex multiplex technology. Meanwhile, mature M2 macrophages secreted multiple growth factors and EVs to transmit a stimulatory signal and reconstruct the regenerative microenvironment (Fig. 3E). The cytokine levels in the M2-C were quantified by ELISA after 72 h of cell culture. VEGF and IL-10 had higher concentrations than the other cytokines (Fig. 3F). The rheological analysis demonstrated that the encapsulation of cytokines did not significantly change the hydrogel modulus (Fig. 3G). The peptide hydrogel scaffold was able to encapsulate M2-

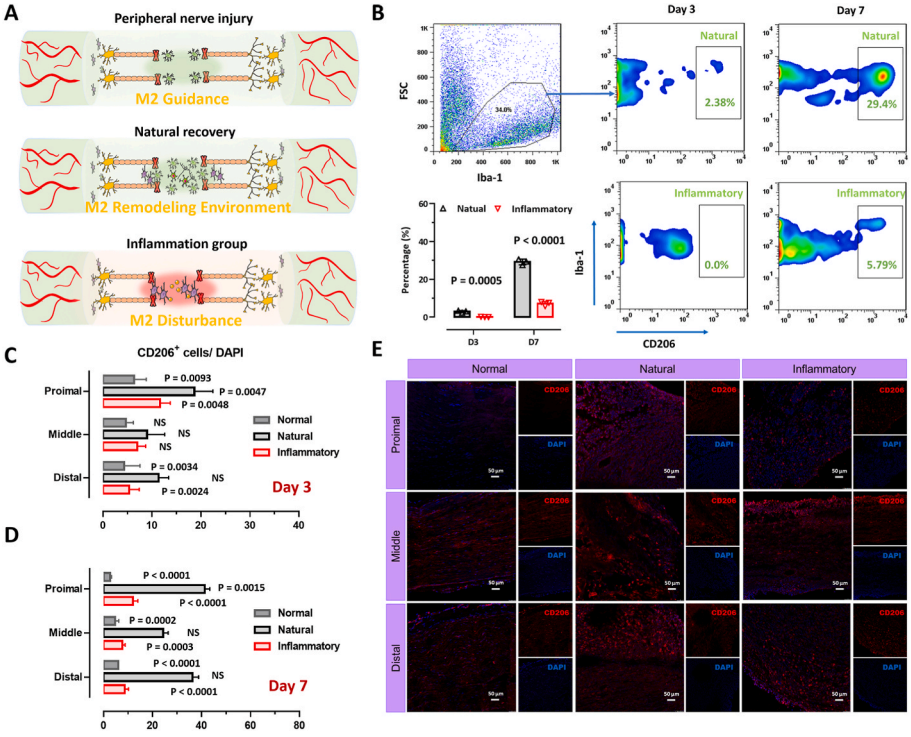

Fig. 1. Local excessive inflammation induced delayed expression of M2. A, Schematic of natural repaired and inflammation group after long-distance peripheral nerve injury. B, Flow cytometry analysis and statistical results the percent of M2 (Iba-1$^+$CD206$^+$) at day 3 and 7 after peripheral nerve defect. The overall experimental process in sciatic nerve gap repaired with a hollow nerve conduit filled with mixed agonist. C-E, The immunofluorescence analysis and statistical the percent of M2 (CD206$^+$) at day 3 (C) and 7 (D-E) after peripheral nerve defect. The values represent mean ± S.D. from at least three independent experiments, and statistical significance was determined by an unpaired two-tailed student's t-test relative to natural group (B), or by a one-way ANOVA with multiple comparisons (C, D) (P values indicated when significant). NS, not significant.

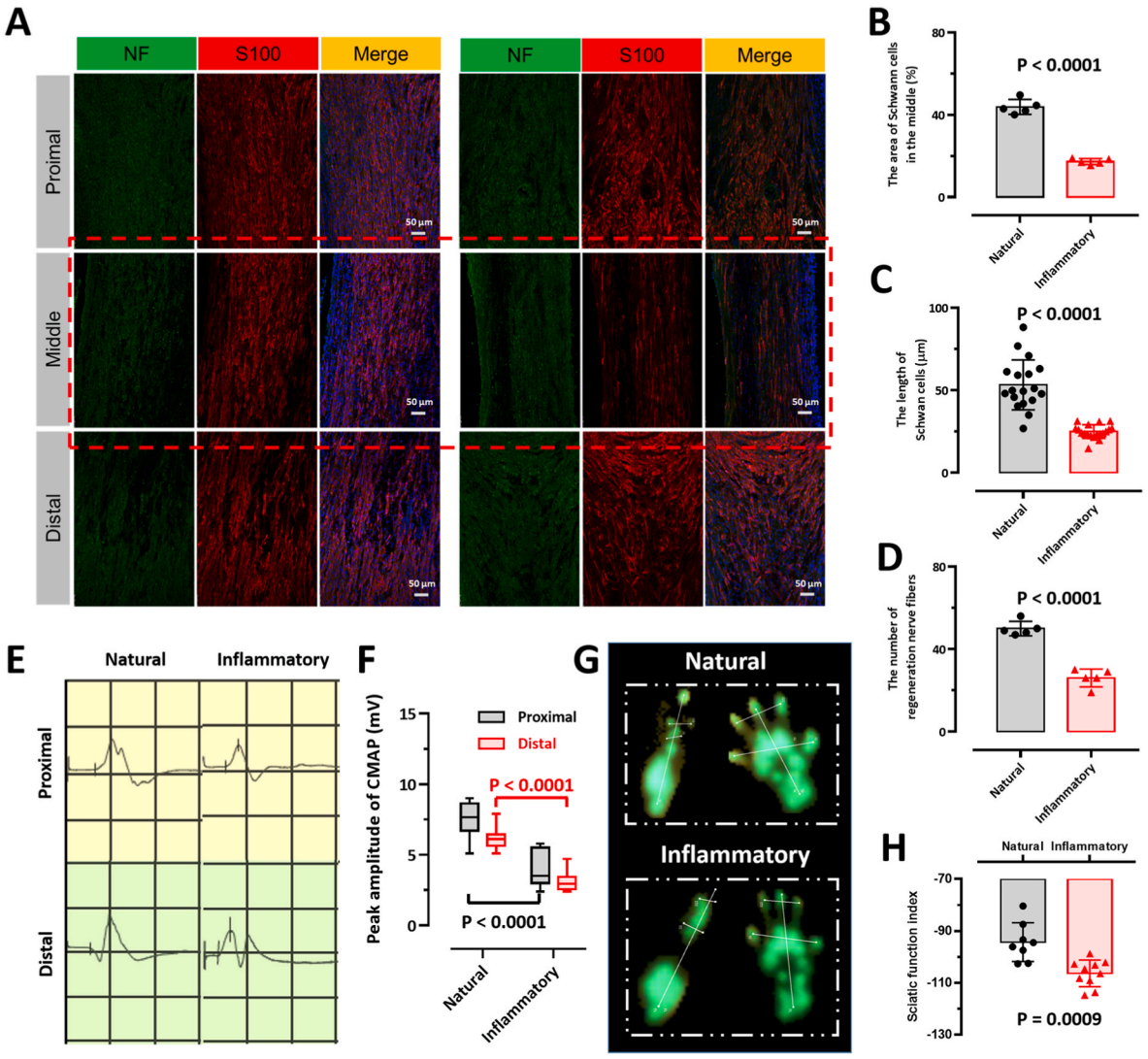

Fig. 2. Local excessive inflammation delayed the sciatic nerve regeneration and functional recovery. A, Representative immunofluorescent images of the longitudinal sections of natural and mixed agonist group at 2 week post-implantation, showing the distribution of nerve (Tuj-1, green) and Schwann cells (S100, red) within different groups. B-C, Quantification of the area and length of Schwann cells in the middle of bridge. D, Quantification of the number of regenerated nerve fibers. E-F, Representative electromyography and peak amplitude of CMAPs of natural and mixed agonist groups at 8 week post-implantation. G-H, Representative footprint and SFI values at 8 week post-implantation. N > 5 per group. The values represent mean ± S.D. from at least three independent experiments, and statistical significance was determined by an unpaired two-tailed student's t-test relative to natural group (P values indicated when significant).

secreted cytokines forming bionic scaffold (bio-scaffold), and there was an immediate and time-dependent release of cytokines over a 6-day period, activating and sustaining release from the hydrogel and remodeling the local immune environment (Fig. 3H).

The viability of macrophages cultured in the bionic peptide scaffold was not significantly different from that of the control group, suggesting excellent cytocompatibility (Fig. S5). Pro-transform macrophages known as M0 macrophages were cultured on bionic peptide scaffolds to investigate their polarization effects. The control group included peptide scaffold alone (scaffold), M2-conditional and normal medium. As shown in Fig. 3I-L, more CD206$^+$ M2 cells were observed in the bionic peptide scaffold and conditional medium groups than in the control group. It have been shown to promote M0 polarization by releasing multiple cytokines into the microenvironment, and the peptide scaffold contained the BDNF mimic motif induced a polarization efficiency of more than 30%, which further enhanced the phenotypical and functional transformation of macrophages.

3.3. Bionic peptide hydrogel scaffolds enhanced Schwann cell proliferation, migration and dorsal root ganglion (DRG) growth behavior

To determine whether bionic peptide scaffold could influence Schwann cell behavior by remodeling the M2 regenerative microenvironment. The cells were plated in bionic peptide scaffolds and peptide scaffolds alone, grown in M2-conditioned and normal media were used as the control groups. After 48 h, the amount of Edu$^+$ Schwann cells in the bionic peptide scaffold group was 2-fold higher than that in the media group. Relative to the peptide scaffold alone and bionic peptide scaffold groups, there were no notable differences in the amount of Edu$^+$ Schwann cells in the M2-conditional and normal media groups. This result indicated that the BDNF mimic motif played a role to some certain in promoting the proliferation of Schwann cell (Fig. 4A and B). We further evaluated the proportion of Edu$^+$ cells among the DAPI Schwann cells. Fig. 4C shows over a 40% increase in Edu$^+$ Schwann cells in the bionic peptide scaffold group compared to the media group. qRT-PCR analysis revealed that the specific markers GFAP and p75 were significantly up-regulated after culture for 3 days in the bionic peptide scaffold

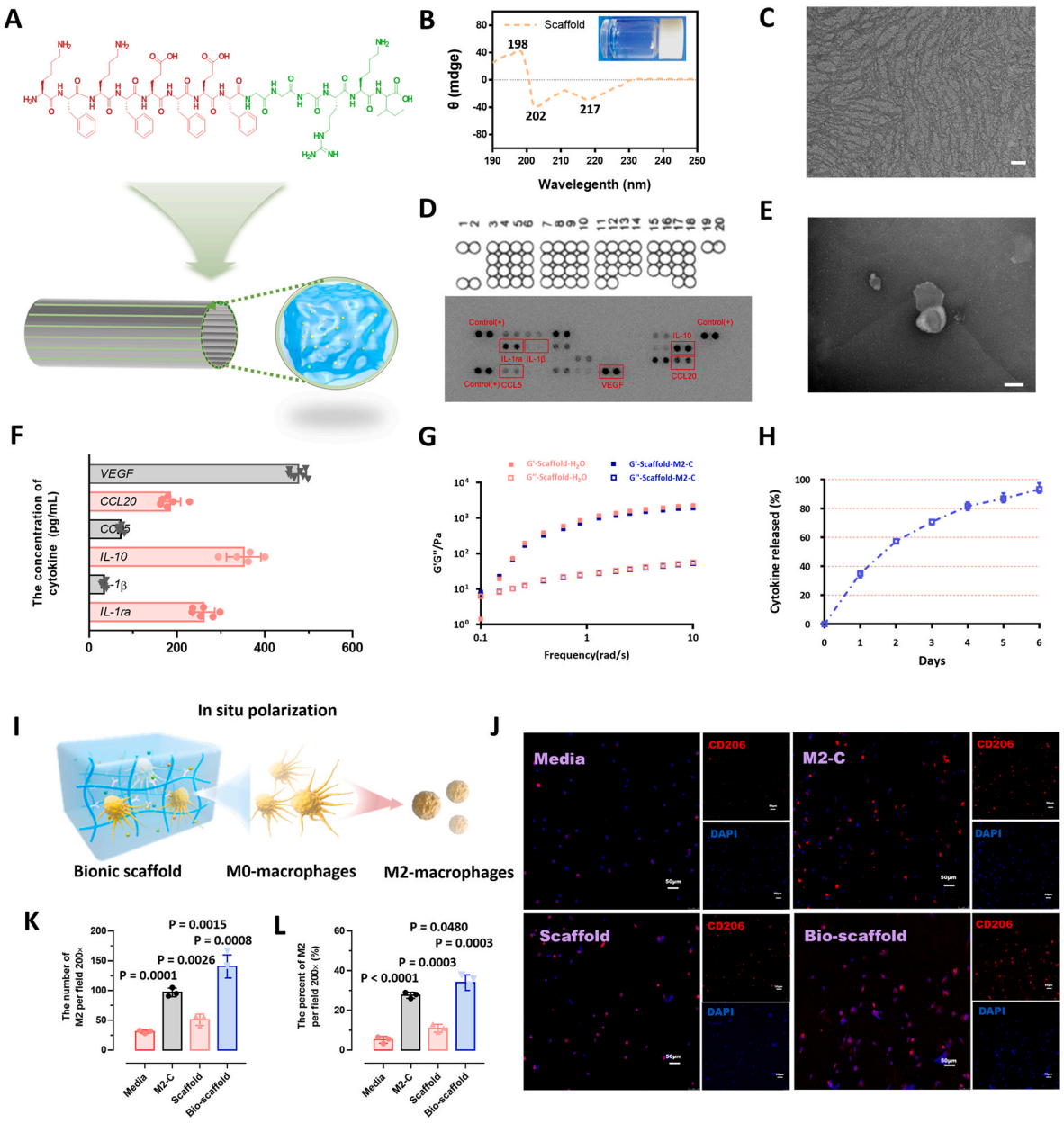

Fig. 3. Generation and characterization of bionic peptide hydrogel scaffold. A, The amino sequence of peptide scaffold and self-assemble into hydrogel. B-C, Circular dichroism (CD) spectra and TEM image of peptide nanofiber. Scale bars = 100 nm. D, Luminex multiplex analysis of M2-conditional media. E, TEM of M2-derived EVs. Scale bars = 100 nm. F, The concentration of M2 secreted cytokines were detected by ELISA. G, Rheological testing of peptide scaffold with H_2O or M2-conditional media. H, The cytokine release profile from the bionic peptide scaffold. Cumulative release was calculated. I, Schematic of bionic peptide scaffold induce M0 macrophages polarization. J, Immunofluorescence of M2 ($CD206^+$, red) was determined by confocal laser scanning microscope. K-L, The number and percent of M2 and results were shown as mean ± S.D. from at least three independent experiments, and statistical significance was determined by a one-way ANOVA with multiple comparisons (P values indicated when significant).

group compared with the other three groups (Fig. 4D and E). The BDNF-related MAPK/ERK signaling pathway was activated by western bolt analysis (Fig. 4F).

Meanwhile, it showed that Schwann cells displayed faster migration in the compatible microenvironment of the bionic peptide scaffold than the other groups at respective time points (Fig. 4G, Fig. S6). In vitro models of neurite outgrowth provide a means to study axonal regeneration potential when DRGs are cultured in different regenerative microenvironments. As shown in Fig. 2H and I, the average lengths of the longest axons in the bionic peptide scaffold (1453.9 ± 113.8 μm), peptide scaffold alone (1150.3 ± 92.7 μm) and M2-conditioned medium (1049.5 ± 63.1 μm) groups were significantly longer than that in the media group (840.1 ± 35.6 μm). In addition, the neurite lengths in the peptide scaffold alone and M2-conditioned medium group were significantly longer than that in the normal medium group, indicating that BDNF and M2-conditioned medium synergistically enhanced neurite outgrowth in vitro.

3.4. *Bionic peptide hydrogel scaffolds promoted macrophage transformation in situ following long-distance peripheral nerve injury*

The effect of bionic peptide hydrogel scaffolds on M2 polarization in situ was investigated using long-distance sciatic nerve injury model. In the natural injury repair process, a large number of M1 macrophages are classically activated to possess proinflammatory, phagocytic, and proteolytic functions essential for damaged tissue digestion and debris

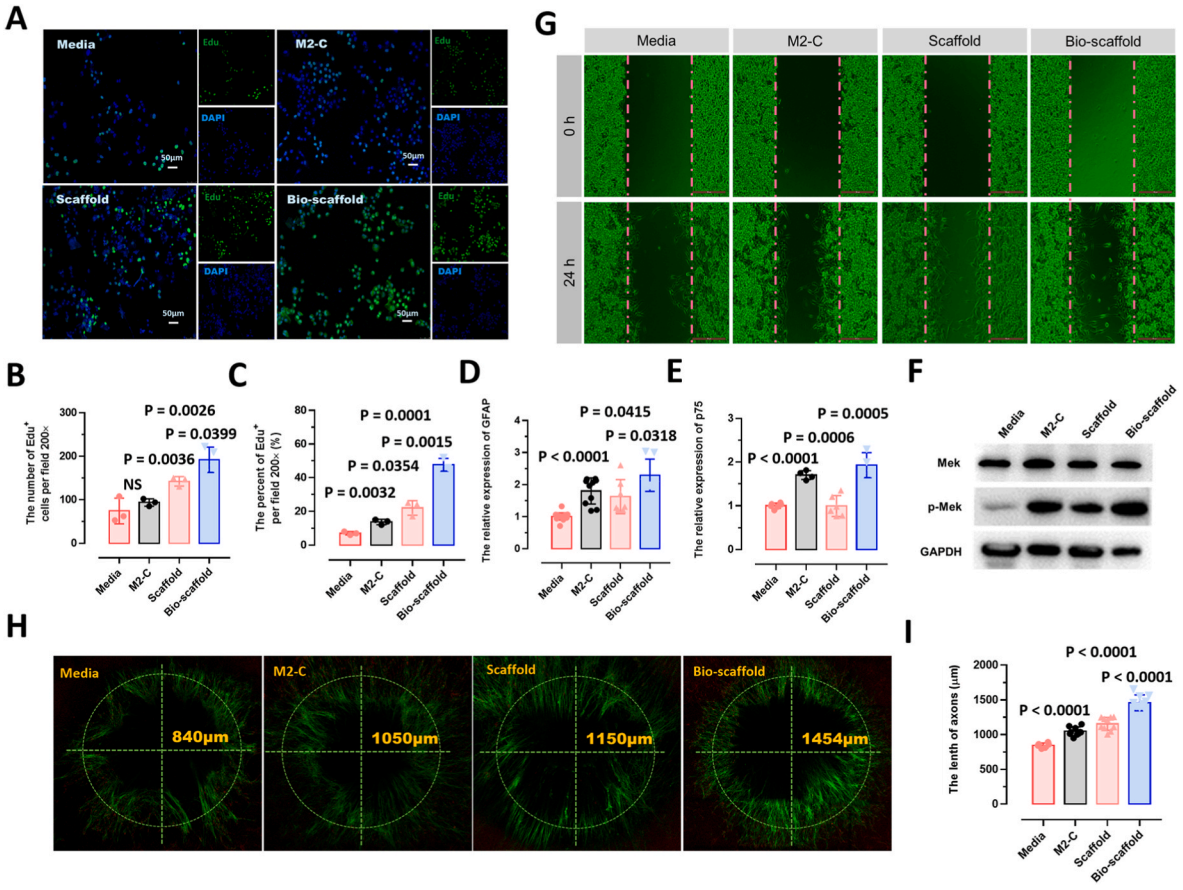

Fig. 4. Bionic peptide hydrogel scaffold regulate Schwann cell proliferation, migration and DRG growth behavior in vitro. A, Representative images of Edu$^+$ Schwann cells (green) in media, M2-conditional media, peptide scaffold and bionic scaffold. B-C, The number and percent of Edu$^+$ Schwann cell. D-E, qRT-PCR analysis of the expression of GFAP and p75. F, Western blot analysis of p-MEK and MEK. G, The migration level of Schwann cell on different microenvironment in the scratch test. H, Fluorescence microscope images of DRG stained with NF200. I, Distribution of longest axons in each group. The results were shown as mean ± S.D. from at least three independent experiments, and statistical significance was determined by a one-way ANOVA with multiple comparisons (P values indicated when significant). NS, not significant.

removal. In this study, the number and proportion of M1 macrophages gradually decreased in the first two weeks, with percentages of 58.4%, 40.2%, 23.8% and 8.66% at day 1, 3, 7 and 14 in the natural repair group, respectively. Correspondingly, 53.3%, 37.8%, 18.2% and 3.5% M1 macrophages were shown in the bionic peptide hydrogel scaffold group at day 1, 3, 7 and 14, respectively. Statistical significance was observed at days 3, 7 and 14, which indicated that the bionic peptide hydrogel scaffold reduced the expression of M1 macrophages to a certain extent (Fig. 5A and B).

M2 macrophages are related to the regeneration of injured nerves, and we detected the efficiency of M2 transformation by the biomimetic local microenvironment. It showed an increase at first and then a decrease in the first two weeks. The percentage of M2 macrophage was 13.7% higher in the bionic peptide hydrogel scaffold compared to the control group at day 7. The percentages of M2 macrophages in the bionic peptide hydrogel scaffold group were 0.98%, 11.4%, 42.2% and 29.9% at day 1, 3, 7, and 14, respectively, showing the same trend as that in the natural repair group (Fig. 5C and D). The bionic peptide hydrogel scaffold regulated the regenerative microenvironment through multiple cytokines to inhibit M1 and promote M2 transformation in a direct and mild manner following long-distance peripheral nerve injury.

3.5. Bionic peptide hydrogel scaffolds promoted nerve regeneration and functional recovery

To determine whether bionic peptide hydrogel in conduits favored nerve regeneration, we further evaluated the implanted scaffolds for 8 week. The peptide scaffold alone, M2-conditional medium, normal medium and autograft groups were used as control. As shown in Fig. 6A, HE and Masson staining of thin sections revealed the presence of a high density of cells and ordered tissue in the bionic peptide hydrogel scaffold and autograft group. However, only sparse and loose cells and tissues were seen in the media group.

Morphological statistical analysis was performed to investigate nerve regeneration in each group. For quantitative analysis of morphometric indices, five sections per sample from the middle of the conduits were examined. The thickness of the myelin sheath from each group was also significantly higher than that of the media group (Fig. 6B). The total number of myelinated axons displayed similar results, but the difference in the M2-conditional medium group was not significant (Fig. 6C). There has been increasingly more attention given to the layer number of myelinated axons from bionic peptide scaffolds, which was comparable to that of autografts and significantly superior to that of the media group (Fig. 6D). The diameter of the regenerative nerve fibers was not significantly different (Fig. 6E). The number and thickness of myelinated axons and the layer number in the bionic peptide scaffold all revealed the faster speed and accuracy of nerve conduction.

To determine the functional recovery of sciatic nerve defects with conduits filled with different scaffolds remodeling the regenerative microenvironment, electrophysiologic testing was performed to evaluate the electrical transduction of regenerated nerves. Representative images in each group are shown in Fig. 7A. The CMAP amplitude were

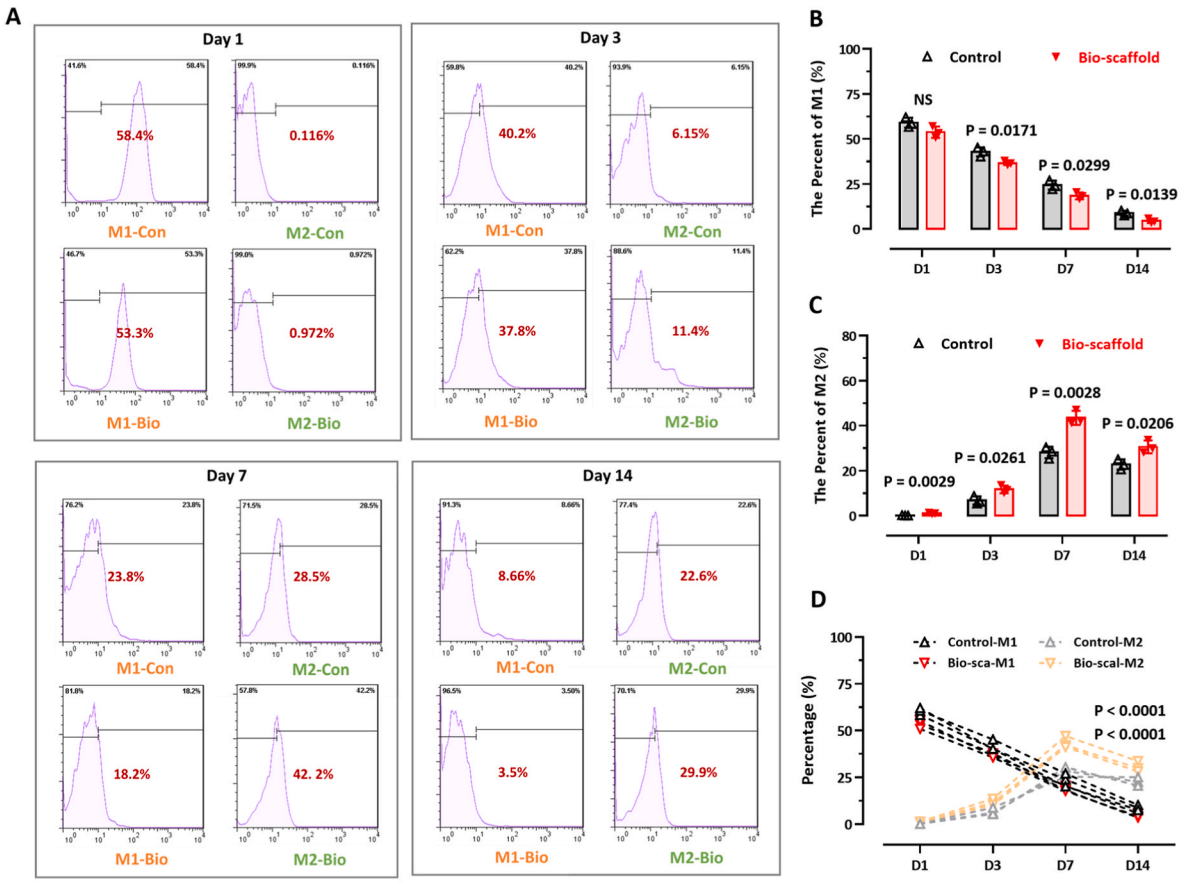

Fig. 5. Bionic peptide hydrogel scaffold promoted M2 transformation in situ following long-distance peripheral nerve injury. A, The representative flow cytometric analysis images of M1 and M2 after bridged with a hollow nerve conduit or the tube filled with bionic peptide hydrogel scaffold. B-D, the corresponding quantification and trend of M1 and M2, and results were shown as mean ± S.D. from at least three independent experiments. The statistical significance was determined by an unpaired two-tailed student's t-test relative to control group (B-C), or by a chi-squared test across all time points (D) (P values indicated when significant). NS, not significant.

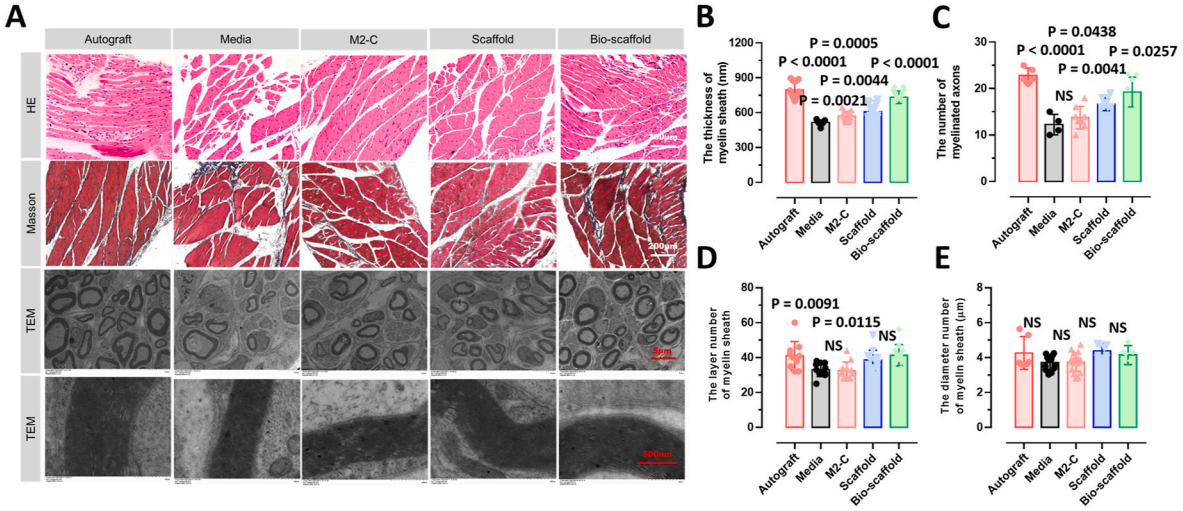

Fig. 6. Morphological statistical analysis of sciatic nerves at 8 week post-implantation. A, HE and Masson staining images of the transverse sections of muscles from the injured limbs. Transmission electron micrographs of regenerated axons and myelin sheath. B, Quantification of the thickness of myelin sheath. C, The number of myelinated axons. D, The layer number of myelinated axons. E, The diameter of myelinated axons. The results were shown as mean ± S.D. from at least three independent experiments, and statistical significance was determined by a one-way ANOVA with multiple comparisons (P values indicated when significant). NS, not significant.

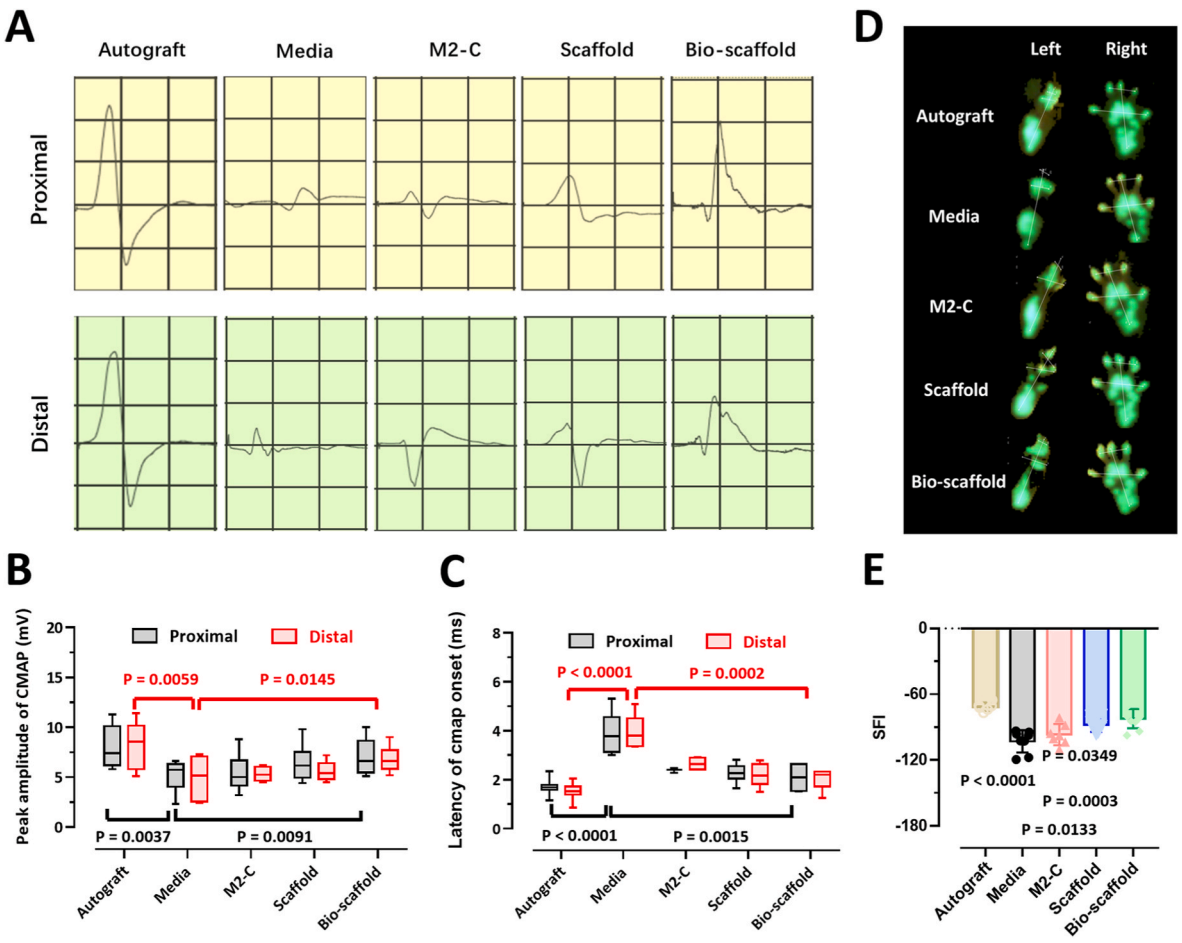

Fig. 7. Bionic peptide hydrogel scaffold showed better functional recovery. A, Representative electromyography of each group at 8 week post-implantation. B, The peak amplitude of CMAP. N > 6 per group. C, The latency of CMAPs oneset. N > 6 per group. D, Representative footprint of each group at 8 week post-implantation. E, SFI values at 8 week post-implantation. The values represent mean ± S.D. from at least three independent experiments, and statistical significance was determined by an unpaired two-tailed student's t-test relative to natural group (P values indicated when significant).

significantly higher in both the proximal and distal ends of the bionic peptide hydrogel scaffold and autograft groups than those in the media group (Fig. 7B). The conduction latency of the group treated with bionic peptide hydrogel scaffold conduits was significantly shorter than that of the media group but still longer than that of the autograft group (Fig. 7C). Footprint assessment was also performed to assess the functional recovery of regenerated nerves (Fig. 7D). The SFI was comparable between bionic peptide hydrogel scaffold and autograft group, and both were significantly higher than that of the media group (Fig. 7E). Overall, it is suggested that BDNF and M2-conditioned medium could work synergistically to promote axonal regeneration and remyelination. However, the autograft still outperformed the bionic peptide hydrogel scaffold.

3.6. Bionic peptide hydrogel scaffolds promoted nerve regeneration following recruitment of blood-derived M2 macrophages

In addition to their role at the injury site, blood monocyte-derived macrophages may play an important role in regeneration. We further combined bionic peptide scaffolds with chemokines targeting blood-derived macrophages to promote nerve regeneration (Fig. 8A). MCP-1 and CX3CL1 are used to recruit M1 and M2 cells, respectively. As shown in Fig. 8B, the total number of macrophages was higher in the bionic peptide scaffold combined with MCP-1 or CX3CL1 group compared to the scaffold only and the control group at day 7 after peripheral nerve defect. Clodronate, an inhibitor of macrophages, can block blood-derived macrophages and reduce their percentage in local scaffold. M2 macrophages were increased due to the recruitment effect of CX3CL1, but there was no significant difference between the MCP-1 and bionic peptide scaffold groups (Fig. 8C).

Muscle structure and function maintenance are also crucial for nerve regeneration. Thus, we evaluated the weight of the gastrocnemius after injury nerve bridged a conduit filled with different scaffold. Gastrocnemius were harvested 8 week after surgery, and the wet weight ratio (injured side/healthy side) was calculated. After injury and repair, the muscle weight showed different degrees of decline in different scaffold group compared to the autograft, and a better recovery effect was noticed in the CX3CL1 group (Fig. 8D and E). Blood-derived M2-marcophage, which recruited by CX3CL1, further promoted the muscle recovery compared to the bionic peptide scaffold ($P = 0.0059$). The morphology of the gastrocnemius was consistent with the observations by HE and masson staining. The CMAP amplitude were significantly higher in both the proximal and distal ends of the M2 recruitment group than those in the bionic peptide scaffold group. The inhibitor group exhibited a weaker signal, suggesting that blood-derived macrophages play a crucial role in nerve regeneration (Fig. 8F). Footprint assessment was also used to evaluate the functional recovery of regenerated nerves. SFI were significantly higher in the M2 recruitment groups than those in the bionic peptide scaffold and inhibitor group (Fig. 8G). These results demonstrated that bionic peptide scaffold combined with CX3CL1 further improved the recovery of injured nerves by recruiting M2 macrophages from the blood.

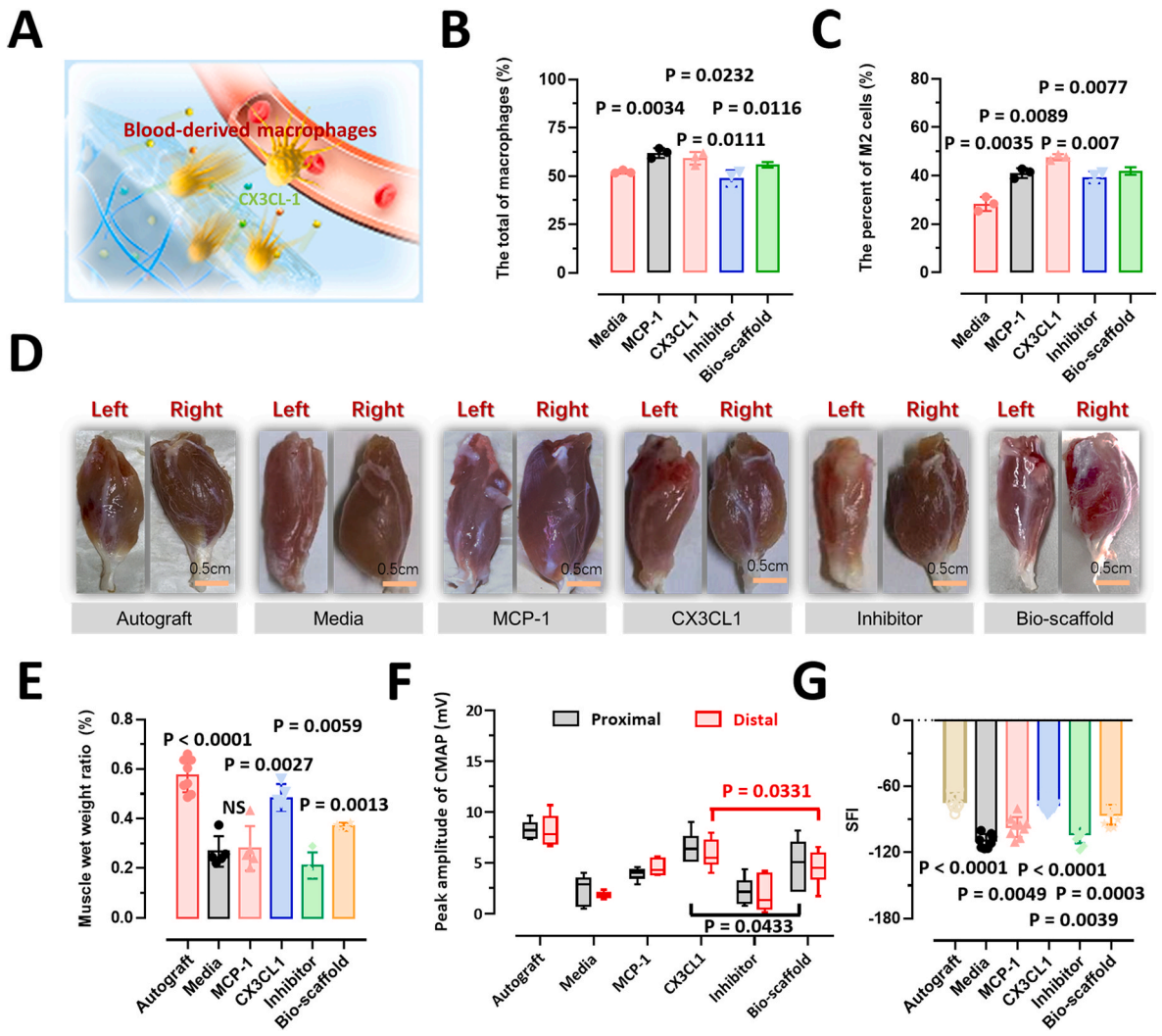

Fig. 8. The chemokines recruit blood monocyte-derived M2 improved functional recovery of injuried sciatic nerve. A, Schematic of chemokines induce macrophages recruitment. B, The total of macrophages and C, The percent of M2 after bridged with nerve conduit filled with bionic peptide hydrogel scaffold encapsulated chemokines. D, Photographs (left: injured side; right: healthy side) and E, Wet gastrocnemius weight ratio. $N > 6$ per group. F, The peak amplitude of CMAP. G, SFI values at 8 week post-implantation. The values represent mean ± S.D. from at least three independent experiments, and statistical significance was determined by a one-way ANOVA with multiple comparisons (B, C, E, G), or by an unpaired two-tailed student's t-test relative to bionic peptide scaffold group (F) (P values indicated when significant). NS, not significant.

4. Discussion

4.1. Model 1

During the process of tissue injury and repair, M2-macrophages participated in the reconstruction of immune microenvironment, which is critical part of the local regenerative microenvironment. A massive number of studies have uncovered the important regulatory effect of macrophages. But, it remains unclear whether the regulative effect is a consequence or a cause. Macrophages was polarized into M2-type as a sign and result of tissue regeneration revealing in previous studies [12,23]. In this study, we firstly concerned whether M2-macrophages become a trigger not just the consequent for regenerative microenvironment. The short-distance peripheral nerve injury can repair itself via the guidance of macrophages [15,24]. In contrast, the endogenous regenerative ability is insufficient in large segments or long distances of nerve defects. The typical rat sciatic nerve in our study was approximately 1.2–1.8 mm in diameter, with a 100–200 μm epineurial and perineurial sheath between the actual axons and the nerve surface [10,25]. We constructed a gap of exceeding at least 4-times of the diameter, which does not permit the end of stumps to be rejoined spontaneously. Local excessive inflammation generated by the mixed agonist reduced the total percentage of M2 macrophages with Iba-1 and CD206 labeling in the bridge. Iba-1 and CD206 are monocyte-macrophage differentiation and typical M2-type macrophage markers, respectively. This state of impaired neurogenesis was coupled with a robust inflammatory response that persists in damaged region. After two weeks, the middle of the regenerative bridge showed a lower fluorescence intensity of newly formed tissue, which was positively correlated with M2-macrophages in the inflammation group. These results verify the guidance and repair role of M2-macrophages, not mix-type macrophages, in long-distance peripheral nerve injury. M2-macrophages could be used as a trigger for remodeling regenerative microenvironment.

4.2. Model 2

The biological activities and functions of regenerative structural cells rely on the 3D scaffold, which provides necessary physical support and biological signals [26,27]. The guidance effect of M2-macrophages is dictated by their interactions with the extracellular matrix (ECM) in 3D structures [28]. Peptide-based materials have shown great promise for

injured nerve regeneration because of their capacity to mimic the structure and complexity of ECM by manipulating the self-assembly of sequences [29,30]. Previous research found that RADA16 and derivatives could support neutrite growth and active synapse formation when sympathetic neurons were cultured [31]. Other peptide hydrogels based on the same self-assembling mechanism have shown good biocompatibility for multiple tissues regeneration [13,32].

In this study, peptide FEFK was applied as a self-assembly scaffold, and it had tunable mechanical properties, could be degraded without adverse effects, and was a platform for the incorporation of bioactive cues [33]. In our previous studies, FEFK displayed excellent performance for rapid proliferation and functional maintenance of immune cells [34]. The flanking domains of FEFK were designed by incorporating the identified BDNF mimic peptide IKRG forming nanoartificial neurotrophic factor, which promoted rapid regeneration of injured nerves [35,36]. Previously published studies applying another BDNF mimetic, RGIDKRHWNSQ, combined with VEGF mimetic have shown similar neurotrophic effects [31]. The mimetic motif is designed based on the solvent-exposed loops 3 and 4 of BDNF, and it can promote neurotrophy and neurite outgrowth by binding to the p75 NTR and TrkB receptors. In this research, the scaffold group only promoted the proliferation and migration of Schwann cells and neuron growth but showed no significant change in macrophage polarization in vitro.

The cell-conditioned medium is composed of secreted cytokines and metabolites, which establish local and systemic microenvironments. Tumor-derived conditioned medium closely mimics the immunosuppressive microenvironment [37]. In contrast, stem cell-conditioned medium can be used for regenerative medicine [2,38]. In this study, M2-derived conditioned medium was used to construct a bionic hydrogel scaffold to mimic the microenvironment of guidance, which is suitable for M2 vitality and nerve regeneration. Cytokines and EVs may serve this function in a quantitative manner, and we detected the types of cytokines and their expression levels to accurately evaluate the repair effect. The certified regenerative cytokines VEGF, IL-10, CCL-20, and CCL-5 were highly expressed in M2-derived conditioned medium, which may help elucidate the mechanism of guidance by M2-macrophages.

It is accepted that M2 polarization is closely related to tissue regeneration; however, few studies have studied the process in a direct way. Disturbances in M2 function can lead to aberrant repair, with uncontrolled inflammatory mediator and growth factor production, deficient generation of anti-inflammatory macrophages, or failed communication between macrophages and epithelial cells, endothelial cells, fibroblasts, and stem or tissue progenitor cells, all contributing to a state of persistent injury, which may lead to the development of pathological fibrosis [22,39]. In the process of macrophage polarization, M1-inflammation and M2-regeneration are interdependent and overlapping phases. Considering the time and rate of macrophage transformation, precise regulation of polarization process is still extremely difficult at present. Many previous research regulated the procession of macrophage polarization by application and design of various biomaterials, but these strategies are indirect and rough. We concerned whether the immune cells derivatives be used as bioactive materials regulating macrophage polarization in a mild manner. In this research, M2-derived condition medium was used to constructed scaffold, which contained multiple cytokines and EVs. The self-assembly peptide scaffold was composed of amino acids completely, which not induced immune response and could be degraded without adverse effects. The forming bionic scaffold remodeled the local microenvironment and regulated M2 macrophages in a direct and mild manner, while the transformation rate was displayed to a certain.

4.3. Model 3

There are two classes of macrophages, resident and infiltrating macrophages, in peripheral nerve tissue. They are distinguishable, but evidence exists that these two types of macrophage perform different functions [12,15,40]. After nerve injury, resident macrophages are quickly activated and phagocytize damage-associated molecular patterns (DAMPs) [41]. Proliferation of resident macrophages also occurs at this early time point, but the quantity cannot meet the demand. Resident macrophages are replaced by circulating monocytes in the later stage of injury, and they become infiltrating macrophages [15]. Whether monocyte-derived macrophages are essential for the clearance of myelin and axonal debris is still controversial, but it is commonly stated that infiltrating macrophages play an important role in the regeneration stage.

For long-distance nerve injury, the prolonged inflammation and regeneration stage requires more macrophages to perform their function. We imitated the recruitment effect of blood-derived macrophages in the body. CX3CR1, as a marker of M2 macrophages, is expressed in monocytes or macrophages during inflammatory conditions [42]. Previous studies have shown that blood-derived M2-macrophages ($Ly6c^{low}CX3CR1^{high}$) function via VCAM-1-VLA-4 adhesion molecules and epithelial CD73 enzymes for extravasation and epithelial transmigration [40,43]. In this study, the bionic peptide hydrogel scaffold combined with CX3CL1, the receptor of CX3CR1, recruited more M2 macrophages targeting the injured nerve. More blood-derived M2 and better recovery of injured nerves were observed in our model. However, the precise process of M2 recruitment and transformation by engineering technology will have to be verified in further studies.

5. Conclusion

M2-macrophages promoted the short-distance peripheral nerve regeneration, however it remains unclear whether the regulative effect is a consequence or a cause. In this study, we firstly confirmed the important role of M2 in guiding and repairing the long-distance peripheral nerve. A bionic peptide hydrogel scaffold based on self-assembly was developed to envelop M2-derived regenerative cytokines and EVs. The regenerative cytokines and EVs were quantified to mimic the immune microenvironment in a direct and mild manner. This bionic peptide hydrogel scaffold remodeled the local environment for M2 transformation and recruitment, favoring long-distance peripheral nerve regeneration. It can help to explicate regulative effect of M2 may be a cause not just a consequence in nerve repair and tissue integration, which facilitating the development of pro-regenerative biomaterials.

Ethics approval and consent to participate

All animal experiments were approved by the Ethics Committee of Nantong University (Nantong, China; approval No. SYXK (SU) 2017-0046). All authors were compliance with all relevant ethical regulations.

Funding

We want to acknowledge the financial support received from the National Natural Science Foundation of China (No. 32230057, 32271389, 31900987), Jiangsu Natural Science Foundation (No. BK20200974), Heilongjiang Natural Science Foundation (No. YQ2019H022), Shuangchuang Program of Jiangsu Province (No. JSSCBS20211603), Nantong Municipal Commission of Health and Family Planning (No. MB2021011), Nantong Science and Technology Plan Project (No. MSZ2022196), Nantong Science and Technology Plan Project (No. JC2019146) and Nantong University Clinical Medicine Project (No. 2019JZ004).

CRediT authorship contribution statement

Pengxiang Yang: Conceptualization, Methodology, Funding acquisition, Writing - original draft, Writing - review & editing. **Yong Peng:** Investigation, Data curation, Validation. **Xiu Dai:** Formal analysis, Funding acquisition. **Jing Jie:** Formal analysis, Writing – review &

editing, Funding acquisition. **Deling Kong:** Formal analysis, Methodology. **Xiaosong Gu:** Project administration, Supervision. **Yumin Yang:** Funding acquisition, Project administration, Writing - review & editing.

Declaration of competing interest

No conflicts of interest exist related to the submission of this manuscript.

Appendix A. Supplementary data

Supplementary data to this article can be found online at https://doi.org/10.1016/j.bioactmat.2023.07.003.

References

[1] B. Liu, W. Xin, J.R. Tan, R.P. Zhu, T. Li, D. Wang, S.S. Kan, D.K. Xiong, H.H. Li, M. M. Zhang, H.H. Sun, W. Wagstaff, C. Zhou, Z.J. Wang, Y.G. Zhang, T.C. He, Myelin sheath structure and regeneration in peripheral nerve injury repair, Proc. Natl. Acad. Sci. U.S.A. 116 (44) (2019) 22347–22352.

[2] X. Li, Y. Guan, C. Li, T. Zhang, F. Meng, J. Zhang, J. Li, S. Chen, Q. Wang, Y. Wang, J. Peng, J. Tang, Immunomodulatory effects of mesenchymal stem cells in peripheral nerve injury, Stem Cell Res. Ther. 13 (1) (2022) 18.

[3] R. Tan, R.K. Krueger, M.J. Gramelspacher, X. Zhou, Y. Xiao, A. Ke, Z. Hou, Y. Zhang, Cas11 enables genome engineering in human cells with compact CRISPR-Cas3 systems, Mol. Cell 82 (4) (2022) 852–867.e5.

[4] Y. Feng, Y. Peng, J. Jie, Y. Yang, P. Yang, The immune microenvironment and tissue engineering strategies for spinal cord regeneration, Front. Cell. Neurosci. 16 (2022), 969002.

[5] D. Ma, H. Shen, F. Chen, W. Liu, Y. Zhao, Z. Xiao, X. Wu, B. Chen, J. Lu, D. Shao, J. Dai, Inflammatory microenvironment-responsive nanomaterials promote spinal cord injury repair by targeting IRF5, Adv. Healthcare Mater. 11 (23) (2022), e2201319.

[6] X. Gu, F. Ding, D.F. Williams, Neural tissue engineering options for peripheral nerve regeneration, Biomaterials 35 (24) (2014) 6143–6156.

[7] S. Wang, C. Zhu, B. Zhang, J. Hu, J. Xu, C. Xue, S. Bao, X. Gu, F. Ding, Y. Yang, X. Gu, Y. Gu, BMSC-derived extracellular matrix better optimizes the microenvironment to support nerve regeneration, Biomaterials 280 (2022), 121251.

[8] A.L. Cattin, J.J. Burden, L. Van Emmenis, F.E. Mackenzie, J.J. Hoving, N. Garcia Calavia, Y. Guo, M. McLaughlin, L.H. Rosenberg, V. Quereda, D. Jamecna, I. Napoli, S. Parrinello, T. Enver, C. Ruhrberg, A.C. Lloyd, Macrophage-induced blood vessels guide schwann cell-mediated regeneration of peripheral nerves, Cell 162 (5) (2015) 1127–1139.

[9] M.D. Park, A. Silvin, F. Ginhoux, M. Merad, Macrophages in health and disease, Cell 185 (23) (2022) 4259–4279.

[10] J.A. Stratton, A. Holmes, N.L. Rosin, S. Sinha, M. Vohra, N.E. Burma, T. Trang, R. Midha, J. Biernaskie, Macrophages regulate schwann cell maturation after nerve injury, Cell Rep. 24 (10) (2018) 2561–2572.e6.

[11] Q. Quan, L. Hong, Y. Wang, R. Li, X. Yin, X. Cheng, G. Liu, H. Tang, H. Meng, S. Liu, Q. Guo, B. Lai, Q. Zhao, M. Wei, J. Peng, P. Tang, Hybrid material mimics a hypoxic environment to promote regeneration of peripheral nerves, Biomaterials 277 (2021), 121068.

[12] J. Li, Y. Yao, Y. Wang, J. Xu, D. Zhao, M. Liu, S. Shi, Y. Lin, Modulation of the crosstalk between schwann cells and macrophages for nerve regeneration: a therapeutic strategy based on a multifunctional tetrahedral framework nucleic acids system, Adv. Mater. (Deerfield Beach, Fla.) 34 (46) (2022), e2202513.

[13] Y. Yan, R. Yao, J. Zhao, K. Chen, L. Duan, T. Wang, S. Zhang, J. Guan, Z. Zheng, X. Wang, Z. Liu, Y. Li, G. Li, Implantable nerve guidance conduits: material combinations, multi-functional strategies and advanced engineering innovations, Bioact. Mater. 11 (2022) 57–76.

[14] K.R. Jessen, P. Arthur-Farraj, Repair Schwann cell update: adaptive reprogramming, EMT, and stemness in regenerating nerves, Glia 67 (3) (2019) 421–437.

[15] P. Liu, J. Peng, G.H. Han, X. Ding, S. Wei, G. Gao, K. Huang, F. Chang, Y. Wang, Role of macrophages in peripheral nerve injury and repair, Neural Regener. Res. 14 (8) (2019) 1335–1342.

[16] S.H. Zhang, G.V. Shurin, H. Khosravi, R. Kazi, O. Kruglov, M.R. Shurin, Y. L. Bunimovich, Immunomodulation by Schwann cells in disease, Cancer Immunol. Immunother. 69 (2) (2020) 245–253.

[17] X. Dong, S. Liu, Y. Yang, S. Gao, W. Li, J. Cao, Y. Wan, Z. Huang, G. Fan, Q. Chen, H. Wang, M. Zhu, D. Kong, Aligned microfiber-induced macrophage polarization to guide schwann-cell-enabled peripheral nerve regeneration, Biomaterials 272 (2021), 120767.

[18] T. Ma, Y. Hao, S. Li, B. Xia, X. Gao, Y. Zheng, L. Mei, Y. Wei, C. Yang, L. Lu, Z. Luo, J. Huang, Sequential oxygen supply system promotes peripheral nerve regeneration by enhancing Schwann cells survival and angiogenesis, Biomaterials 289 (2022), 121755.

[19] J.T. Reeder, Z. Xie, Q. Yang, M.H. Seo, Y. Yan, Y. Deng, K.R. Jinkins, S.R. Krishnan, C. Liu, S. McKay, E. Patnaude, A. Johnson, Z. Zhao, M.J. Kim, Y. Xu, I. Huang, R. Avila, C. Felicelli, E. Ray, X. Guo, W.Z. Ray, Y. Huang, M.R. MacEwan, J. A. Rogers, Soft, bioresorbable coolers for reversible conduction block of peripheral nerves, Science (New York, N.Y.) 377 (6601) (2022) 109–115.

[20] Y. Qian, H. Lin, Z. Yan, J. Shi, C. Fan, Functional nanomaterials in peripheral nerve regeneration: scaffold design, chemical principles and microenvironmental remodeling, Mater. Today 51 (2021) 165–187.

[21] R. Wang, X. Wu, Z. Tian, T. Hu, C. Cai, G. Wu, G.B. Jiang, B. Liu, Sustained release of hydrogen sulfide from anisotropic ferrofluid hydrogel for the repair of spinal cord injury, Bioact. Mater. 23 (2023) 118–128.

[22] T.A. Wynn, K.M. Vannella, Macrophages in tissue repair, regeneration, and fibrosis, Immunity 44 (3) (2016) 450–462.

[23] C. Zhang, D. Li, H. Hu, Z. Wang, J. An, Z. Gao, K. Zhang, X. Mei, C. Wu, H. Tian, Engineered extracellular vesicles derived from primary M2 macrophages with anti-inflammatory and neuroprotective properties for the treatment of spinal cord injury, J. Nanobiotechnol. 19 (1) (2021) 373.

[24] R.E. Zigmond, F.D. Echevarria, Macrophage biology in the peripheral nervous system after injury, Prog. Neurobiol. 173 (2019) 102–121.

[25] L. Zhu, K. Wang, T. Ma, L. Huang, B. Xia, S. Zhu, Y. Yang, Z. Liu, X. Quan, K. Luo, D. Kong, J. Huang, Z. Luo, Noncovalent bonding of RGD and YIGSR to an electrospun poly(epsilon-caprolactone) conduit through peptide self-assembly to synergistically promote sciatic nerve regeneration in rats, Adv. Healthcare Mater. 6 (8) (2017).

[26] T. Lin, S. Liu, S. Chen, S. Qiu, Z. Rao, J. Liu, S. Zhu, L. Yan, H. Mao, Q. Zhu, D. Quan, X. Liu, Hydrogel derived from porcine decellularized nerve tissue as a promising biomaterial for repairing peripheral nerve defects, Acta Biomater. 73 (2018) 326–338.

[27] P. Yang, H. Song, Y. Qin, P. Huang, C. Zhang, D. Kong, W. Wang, Engineering dendritic-cell-based vaccines and PD-1 blockade in self-assembled peptide nanofibrous hydrogel to amplify antitumor T-cell immunity, Nano Lett. 18 (7) (2018) 4377–4385.

[28] Z. Yu, Z. Cai, Q. Chen, M. Liu, L. Ye, J. Ren, W. Liao, S. Liu, Engineering beta-sheet peptide assemblies for biomedical applications, Biomater. Sci. 4 (3) (2016) 365–374.

[29] T.L. Lopez-Silva, C.D. Cristobal, C.S. Edwin Lai, V. Leyva-Aranda, H.K. Lee, J. D. Hartgerink, Self-assembling multidomain peptide hydrogels accelerate peripheral nerve regeneration after crush injury, Biomaterials 265 (2021), 120401.

[30] M. Dergham, S. Lin, J. Geng, Supramolecular self-assembly in living cells, Angew. Chem. Int. Ed. 61 (18) (2022), e202114267.

[31] J. Lu, X. Yan, X. Sun, X. Shen, H. Yin, C. Wang, Y. Liu, C. Lu, H. Fu, S. Yang, Y. Wang, X. Sun, L. Zhao, S. Lu, A.G. Mikos, J. Peng, X. Wang, Synergistic effects of dual-presenting VEGF- and BDNF-mimetic peptide epitopes from self-assembling peptide hydrogels on peripheral nerve regeneration, Nanoscale 11 (42) (2019) 19943–19958.

[32] N. Yadav, M.K. Chauhan, V.S. Chauhan, Short to ultrashort peptide-based hydrogels as a platform for biomedical applications, Biomater. Sci. 8 (1) (2020) 84–100.

[33] P. Yang, H. Song, Z. Feng, C. Wang, P. Huang, C. Zhang, D. Kong, W. Wang, Synthetic, supramolecular, and self-adjuvanting cd8+t-cell epitope vaccine increases the therapeutic antitumor immunity, Adv. Therapeut. 2 (7) (2019), 1900010.

[34] J. Jie, D. Mao, J. Cao, P. Feng, P. Yang, Customized multifunctional peptide hydrogel scaffolds for CAR-T-cell rapid proliferation and solid tumor immunotherapy, ACS Appl. Mater. Interfaces 14 (33) (2022) 37514–37527.

[35] K. Kulkarni, R.L. Minehan, T. Gamot, H.A. Coleman, S. Bowles, Q. Lin, D. Hopper, S.E. Northfield, R.A. Hughes, R.E. Widdop, M.I. Aguilar, H.C. Parkington, M.P. Del Borgo, Esterase-mediated sustained release of peptide-based therapeutics from a self-assembled injectable hydrogel, ACS Appl. Mater. Interfaces 13 (49) (2021) 58279–58290.

[36] A.N. Edelbrock, Z. Àlvarez, D. Simkin, T. Fyrner, S.M. Chin, K. Sato, E. Kiskinis, S. I. Stupp, Supramolecular nanostructure activates TrkB receptor signaling of neuronal cells by mimicking brain-derived neurotrophic factor, Nano Lett. 18 (10) (2018) 6237–6247.

[37] P. Yang, X. Cao, H. Cai, X. Chen, Y. Zhu, Y. Yang, W. An, J. Jie, Upregulation of microRNA-155 enhanced migration and function of dendritic cells in three-dimensional breast cancer microenvironment, Immunol. Invest. 50 (8) (2021) 1058–1071.

[38] C. De Gregorio, D. Contador, D. Díaz, C. Cárcamo, D. Santapau, L. Lobos-Gonzalez, C. Acosta, M. Campero, D. Carpio, C. Gabriele, M. Gaspari, V. Aliaga-Tobar, V. Maracaja-Coutinho, M. Ezquer, F. Ezquer, Human adipose-derived mesenchymal stem cell-conditioned medium ameliorates polyneuropathy and foot ulceration in diabetic BKS db/db mice, Stem Cell Res. Ther. 11 (1) (2020) 168.

[39] G. Xiang, K. Liu, T. Wang, X. Hu, J. Wang, Z. Gao, W. Lei, Y. Feng, T.H. Tao, In situ regulation of macrophage polarization to enhance osseointegration under diabetic conditions using injectable silk/sitagliptin gel scaffolds, Adv. Sci. 8 (3) (2021), 2002328.

[40] R. Shechter, O. Miller, G. Yovel, N. Rosenzweig, A. London, J. Ruckh, K.W. Kim, E. Klein, V. Kalchenko, P. Bendel, S.A. Lira, S. Jung, M. Schwartz, Recruitment of beneficial M2 macrophages to injured spinal cord is orchestrated by remote brain choroid plexus, Immunity 38 (3) (2013) 555–569.

[41] A. Boissonnas, F. Louboutin, M. Laviron, P.L. Loyher, E. Reboussin, S. Barthelemy, A. Reaux-Le Goazigo, C.S. Lobsiger, B. Combadiere, S. Melik Parsadaniantz,

C. Combadiere, Imaging resident and recruited macrophage contribution to Wallerian degeneration, J. Exp. Med. 217 (11) (2020).
[42] N. Yoshiba, N. Edanami, N. Ohkura, T. Maekawa, N. Takahashi, A. Tohma, K. Izumi, T. Maeda, A. Hosoya, H. Nakamura, K. Tabeta, Y. Noiri, K. Yoshiba, M2 phenotype macrophages colocalize with schwann cells in human dental pulp, J. Dent. Res. 99 (3) (2020) 329–338.
[43] S.F. Ma, Y.J. Chen, J.X. Zhang, L. Shen, R. Wang, J.S. Zhou, J.G. Hu, H.Z. Lü, Adoptive transfer of M2 macrophages promotes locomotor recovery in adult rats after spinal cord injury, Brain Behav. Immun. 45 (2015) 157–170.